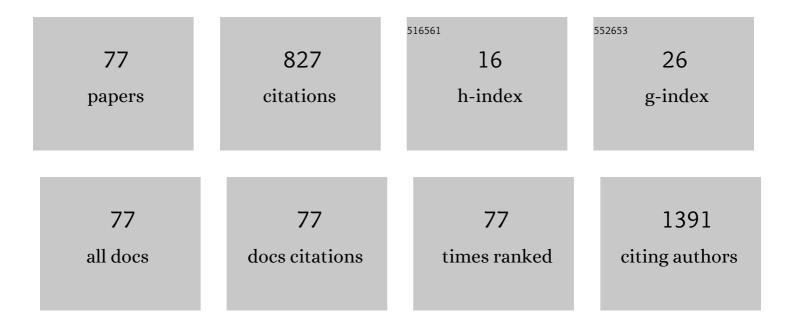
List of Publications by Year in descending order

Source: https://exaly.com/author-pdf/3111835/publications.pdf Version: 2024-02-01



#	Article	IF	CITATIONS
1	OUP accepted manuscript. Cerebral Cortex Communications, 2022, 3, tgab064.	0.7	2
2	Targeting brain regions of interest in functional nearâ€infrared spectroscopy—Scalpâ€cortex correlation using subjectâ€specific light propagation models. Human Brain Mapping, 2021, 42, 1969-1986.	1.9	5
3	Correlating functional near-infrared spectroscopy with underlying cortical regions of 0-, 1-, and 2-year-olds using theoretical light propagation analysis. Neurophotonics, 2021, 8, 025009.	1.7	3
4	Functional near-infrared-spectroscopy-based measurement of changes in cortical activity in macaques during post-infarct recovery of manual dexterity. Scientific Reports, 2020, 10, 6458.	1.6	13
5	Exclusive detection of cerebral hemodynamics in functional near-infrared spectroscopy by reflectance modulation of the scalp surface. Journal of Biomedical Optics, 2020, 25, 1.	1.4	1
6	In situ estimation of optical properties of rat and monkey brains using femtosecond time-resolved measurements. Scientific Reports, 2019, 9, 9165.	1.6	12
7	Spatiotemporal dynamics of red blood cells in capillaries in layer I of the cerebral cortex and changes in arterial diameter during cortical spreading depression and response to hypercapnia in anesthetized mice. Microcirculation, 2019, 26, e12552.	1.0	2
8	A fNIRS probe positioning system using augmented reality technology. , 2019, , .		2
9	Time-domain diffuse optical tomography with lp sparsity regularization for thyroid cancer imaging. , 2019, , .		0
10	Comparison of diffusion-weighted MRI and anti-Stokes Raman scattering (CARS) measurements of the inter-compartmental exchange-time of water in expression-controlled aquaporin-4 cells. Scientific Reports, 2018, 8, 17954.	1.6	18
11	Functional near-infrared spectroscopy for monitoring macaque cerebral motor activity during voluntary movements without head fixation. Scientific Reports, 2018, 8, 11941.	1.6	6
12	Partial optical path length in the scalp in subject-specific head models for multi-distance probe configuration of near infrared spectroscopy. , 2018, , .		0
13	Changes in effective diffusivity for oxygen during neural activation and deactivation estimated from capillary diameter measured by two-photon laser microscope. Journal of Physiological Sciences, 2017, 67, 325-330.	0.9	4
14	Design and fabrication of a multi-layered solid dynamic phantom: validation platform on methods for reducing scalp-hemodynamic effect from fNIRS signal. Proceedings of SPIE, 2017, , .	0.8	0
15	Functional near infrared spectroscopy for awake monkey to accelerate neurorehabilitation study. , 2017, , .		2
16	Visual evaluation of kinetic characteristics of PET probe for neuroreceptors using a two-phase graphic plot analysis. Annals of Nuclear Medicine, 2017, 31, 273-282.	1.2	2
17	Normative data of dopaminergic neurotransmission functions in substantia nigra measured with MRI and PET: Neuromelanin, dopamine synthesis, dopamine transporters, and dopamine D2 receptors. NeuroImage, 2017, 158, 12-17.	2.1	19
18	Estimation of functional areas probed by near-infrared spectroscopy instruments. Proceedings of SPIE, 2017, , .	0.8	0

#	Article	IF	CITATIONS
19	Dynamic Flow Velocity Mapping from Fluorescent Dye Transit Times in the Brain Surface Microcirculation of Anesthetized Rats and Mice. Microcirculation, 2016, 23, 416-425.	1.0	9
20	Diffusion-tensor-based method for robust and practical estimation of axial and radial diffusional kurtosis. European Radiology, 2016, 26, 2559-2566.	2.3	9
21	Estimation of partial optical path length in the brain in subject-specific head models for near-infrared spectroscopy. Optical Review, 2016, 23, 316-322.	1.2	10
22	Principal Component Analysis of Multimodal Neuromelanin MRI and Dopamine Transporter PET Data Provides a Specific Metric for the Nigral Dopaminergic Neuronal Density. PLoS ONE, 2016, 11, e0151191.	1.1	27
23	Fluorescence Imaging of Blood Flow Velocity in the Rodent Brain. Current Topics in Medicinal Chemistry, 2016, 16, 2677-2684.	1.0	8
24	Construction of an Anatomical Neck Model for Diffuse Optical Imaging. , 2016, , .		1
25	2F44 Development for mapping the flow velocity dynamics with fluorescent imaging techniques. The Proceedings of the Bioengineering Conference Annual Meeting of BED/JSME, 2016, 2016.28, _2F44-12F44-5	0.0	Ο
26	Unveiling astrocytic control of cerebral blood flow with optogenetics. Scientific Reports, 2015, 5, 11455.	1.6	72
27	Technological Trend of Noninvasive Brain-Function Imaging by Near-Infrared Spectroscopy. Nippon Laser Igakkaishi, 2015, 36, 187-194.	0.0	Ο
28	Hyperperfusion Counteracted by Transient Rapid Vasoconstriction Followed by Long-Lasting Oligemia Induced by Cortical Spreading Depression in Anesthetized Mice. Journal of Cerebral Blood Flow and Metabolism, 2015, 35, 689-698.	2.4	15
29	Magnetic resonance imaging appropriate for construction of subject-specific head models for diffuse optical tomography. Biomedical Optics Express, 2015, 6, 3197.	1.5	7
30	Reconstruction magnetic resonance neurography in chronic inflammatory demyelinating polyneuropathy. Annals of Neurology, 2015, 77, 333-337.	2.8	103
31	Reproducibility of measuring cerebral blood flow by laser-Doppler flowmetry in mice. Frontiers in Bioscience - Elite, 2014, E6, 62-68.	0.9	5
32	Changes in Cortical Microvasculature during Misery Perfusion Measured by Two-Photon Laser Scanning Microscopy. Journal of Cerebral Blood Flow and Metabolism, 2014, 34, 1363-1372.	2.4	22
33	Microvascular Sprouting, Extension, and Creation of New Capillary Connections with Adaptation of the Neighboring Astrocytes in Adult Mouse Cortex under Chronic Hypoxia. Journal of Cerebral Blood Flow and Metabolism, 2014, 34, 325-331.	2.4	27
34	Cerebral hemodynamic response to acute hyperoxia in awake mice. Brain Research, 2014, 1557, 155-163.	1.1	9
35	Signal contributions to heavily diffusion-weighted functional magnetic resonance imaging investigated with multi-SE-EPI acquisitions. NeuroImage, 2014, 98, 258-265.	2.1	7
36	Evaluation of Rho-Kinase Activity in Mice Brain Using N-[11C]Methyl-hydroxyfasudil with Positron Emission Tomography. Molecular Imaging and Biology, 2014, 16, 395-402.	1.3	11

#	Article	IF	CITATIONS
37	Pial Arteries Respond Earlier than Penetrating Arterioles to Neural Activation in the Somatosensory Cortex in Awake Mice Exposed to Chronic Hypoxia: An Additional Mechanism to Proximal Integration Signaling?. Journal of Cerebral Blood Flow and Metabolism, 2014, 34, 1761-1770.	2.4	25
38	A proposal for PET/MRI attenuation correction with μ-values measured using a fixed-position radiation source and MRI segmentation. Nuclear Instruments and Methods in Physics Research, Section A: Accelerators, Spectrometers, Detectors and Associated Equipment, 2014, 734, 156-161.	0.7	7
39	Automated Image Analysis for Diameters and Branching Points of Cerebral Penetrating Arteries and Veins Captured with Two-Photon Microscopy. Advances in Experimental Medicine and Biology, 2014, 812, 209-215.	0.8	5
40	Relation between Dopamine Synthesis Capacity and Cell-Level Structure in Human Striatum: A Multi-Modal Study with Positron Emission Tomography and Diffusion Tensor Imaging. PLoS ONE, 2014, 9, e87886.	1.1	15
41	Path Length Correction in Exposed-Cortex Optical Imaging using 3D Model Obtained by Two-Photon Microscopy. , 2014, , .		0
42	Vessel Specific Imaging of Glucose Transfer with Fluorescent Glucose Analogue in Anesthetized Mouse Cortex. Advances in Experimental Medicine and Biology, 2014, 812, 241-246.	0.8	0
43	A MRI-based PET attenuation correction with μ-values measured by a fixed-position radiation source. , 2013, , .		0
44	Long-Term Adaptation of Cerebral Hemodynamic Response to Somatosensory Stimulation during Chronic Hypoxia in Awake Mice. Journal of Cerebral Blood Flow and Metabolism, 2013, 33, 774-779.	2.4	30
45	Hemodynamic changes during neural deactivation in awake mice: A measurement by laser-Doppler flowmetry in crossed cerebellar diaschisis. Brain Research, 2013, 1537, 350-355.	1.1	16
46	Layer-Specific Dilation of Penetrating Arteries Induced by Stimulation of the Nucleus Basalis of Meynert in the Mouse Frontal Cortex. Journal of Cerebral Blood Flow and Metabolism, 2013, 33, 1440-1447.	2.4	22
47	Effect of probe arrangement on reconstruction of optical brain function imaging. , 2013, , .		0
48	Visualization of microvessels and capillary bed associated with brain activation. , 2013, , .		0
49	Dynamic Two-Photon Imaging of Cerebral Microcirculation Using Fluorescently Labeled Red Blood Cells and Plasma. Advances in Experimental Medicine and Biology, 2013, 765, 163-168.	0.8	3
50	Hypoxia-Induced Cerebral Angiogenesis in Mouse Cortex with Two-Photon Microscopy. Advances in Experimental Medicine and Biology, 2013, 789, 15-20.	0.8	11
51	Measuring the Vascular Diameter of Brain Surface and Parenchymal Arteries in Awake Mouse. Advances in Experimental Medicine and Biology, 2013, 789, 419-425.	0.8	23
52	The influence of frontal sinus in brain activation measurements by near-infrared spectroscopy analyzed by realistic head models. Biomedical Optics Express, 2012, 3, 2121.	1.5	22
53	Hybrid segmentation-atlas method for PET-MRI attenuation correction. , 2012, , .		4
54	Hemodynamic changes during somatosensory stimulation in awake and isoflurane-anesthetized mice measured by laser-Doppler flowmetry. Brain Research, 2012, 1472, 107-112.	1,1	32

#	Article	IF	CITATIONS
55	Image-based vessel-by-vessel analysis for red blood cell and plasma dynamics with automatic segmentation. Microvascular Research, 2012, 84, 178-187.	1.1	10
56	7D22 Quantitative analysis of micro vascular network structure in the cerebral cortex The Proceedings of the Bioengineering Conference Annual Meeting of BED/JSME, 2012, 2012.24, _7D22-17D22-2	0.0	0
57	Analysis of Light Propagation in a Realistic Head Model Including Frontal Sinus. , 2012, , .		Ο
58	Segmentation of magnetic resonance images to construct human head model for diffuse optical imaging. Proceedings of SPIE, 2011, , .	0.8	0
59	Anatomic dependency of phase shifts in the cerebral venous system of neonates at susceptibilityâ€weighted MRI. Journal of Magnetic Resonance Imaging, 2011, 34, 1031-1036.	1.9	5
60	Phantom experiments for quantitative evaluation of topographic image by mapping algorithm. Proceedings of SPIE, 2011, , .	0.8	1
61	Spatial Frequency-Based Analysis of Mean Red Blood Cell Speed in Single Microvessels: Investigation of Microvascular Perfusion in Rat Cerebral Cortex. PLoS ONE, 2011, 6, e24056.	1.1	22
62	Segmentation of magnetic resonance images to construct human head model for diffuse optical imaging. , 2011, , .		0
63	Voxel-based analysis of the diffusion tensor. Neuroradiology, 2010, 52, 699-710.	1.1	59
64	Regional heterogeneity and age-related change in sub-regions of internal capsule evaluated by diffusion tensor imaging. Brain Research, 2010, 1354, 30-39.	1.1	12
65	A Head Phantom for Use in Near Infrared Topography for Brain Function Measurements. , 2010, , .		0
66	Validation of practical diffusion approximation for virtual near infrared spectroscopy using a digital head phantom. Optical Review, 2009, 16, 153-159.	1.2	7
67	Theoretical analysis of crosstalk between oxygenated and deoxygenated haemoglobin in focal brain-activation measurements by near-infrared topography. Opto-electronics Review, 2008, 16, .	2.4	3
68	Normalized Adult Head Model for the Image Reconstruction Algorithm of NIR Topography. , 2008, , .		0
69	Evaluation of image reconstruction algorithm for near infrared topography by virtual head phantom. Proceedings of SPIE, 2007, , .	0.8	2
70	Effect of probe arrangement on reproducibility of images by near-infrared topography evaluated by a virtual head phantom. Applied Optics, 2007, 46, 1658.	2.1	27
71	Virtual Head Phantom for Evaluation of Near Infrared Topography. , 2006, , .		0
72	Image reconstruction using spatial sensitivity profile with the constraint of spatial frequency in image for near-infrared topography. , 2005, , .		0

#	ARTICLE	IF	CITATIONS
73	Image Reconstruction Using Spatial Sensitivity Profile with the Constraint of Spatial Frequency in Image for Near-Infrared Topography. , 2005, , .		0
74	Theoretical evaluation of accuracy in position and size of brain activity obtained by near-infrared topography. Physics in Medicine and Biology, 2004, 49, 2753-2765.	1.6	30
75	<title>Modeling of light distribution in the brain for topographical imaging</title> . , 2004, 5486, 1.		0
76	Evaluation of spatial resolution of near-infrared topography using spatial sensitivity profile. , 2003, 5138, 249.		1
77	Improvement of near-infrared topography by optode arrangement and reconstruction algorithm using spatial sensitivity profile. , 0, , .		0